

See discussions, stats, and author profiles for this publication at: <https://www.researchgate.net/publication/5494452>

Optical Resonance-Enhanced Absorption-Based Near-Field Immuno chip Biosensor for Allergen Detection

ARTICLE in ANALYTICAL CHEMISTRY · MAY 2008

Impact Factor: 5.64 · DOI: 10.1021/ac702107k · Source: PubMed

CITATIONS

38

READS

32

4 AUTHORS, INCLUDING:



Irene Maier

University of Vienna

11 PUBLICATIONS 165 CITATIONS

SEE PROFILE



Wolfgang Lindner

University of Vienna

270 PUBLICATIONS 7,060 CITATIONS

SEE PROFILE



Fritz Pittner

University of Vienna

126 PUBLICATIONS 1,434 CITATIONS

SEE PROFILE

Optical Resonance-Enhanced Absorption-Based Near-Field Immunochip Biosensor for Allergen Detection

Irene Maier,^{*,†,‡} Michael R. A. Morgan,[§] Wolfgang Lindner,^{||} and Fritz Pittner[†]

Max F. Perutz Laboratories, Department of Biochemistry, University of Vienna, Dr. Bohr-Gasse 9, 1030 Vienna, Austria, Procter Department of Food Science, University of Leeds, LS2 9JT, Leeds, UK, and Institute of Analytical Chemistry and Food Chemistry, University of Vienna, Währinger Strasse 38, 1090 Vienna, Austria

An optical immunochip biosensor has been developed as a rapid method for allergen detection in complex food matrixes, and its application evaluated for the detection of the egg white allergens, ovalbumin and ovomucoid. The optical near-field phenomenon underlying the basic principle of the sensor design is called resonance-enhanced absorption (REA), which utilizes gold nanoparticles (Au NPs) as signal transducers in a highly sensitive interferometric setup. Using this approach, a novel, simple, and rapid colorimetric solid-phase immunoassay on a planar chip substrate was realized in direct and sandwich assay formats, with a detection system that does not require any instrumentation for readout. Semiquantitative immunochemical responses are directly visible to the naked eye of the analyst. The biosensor shows concentration-dependent color development by capturing antibody-functionalized Au NPs on allergen-coated chips and has a detection limit of 1 ng/mL. To establish a rapid method, we took advantage of the physicochemical microenvironment of the Au NP–antibody bioconjugate to be bound directly over an interacting poly(styrene–methyl methacrylate) interlayer by an immobilized antigen. In the direct assay format, a coating time with allergen of only 5 min under “soft” nondenaturing conditions was sufficient for accurate reproducibility and sensitivity. In conclusion, the REA-based immunochip sensor is easy to fabricate, is reproducible and selective in its performance, has minimal technical requirements, and will enable high-throughput screening of affinity binding interactions in technological and medical applications.

Recent approaches to quantitatively measure the abundance, state, and differences in states of many proteins precisely and simultaneously in industrial food control, medical diagnosis, and biological research demand a rapid, high-throughput technology to reflect protein characteristics.¹ Since the development of optical

near-field microscopy, optical biosensors have been realized as a method of choice to allow for imaging of biomolecules. However, it was not before measurements started to incorporate the use of metal nanoparticles, which interact with electromagnetic waves of the visible and near-infrared spectrum, that optical investigation of bioanalytes demonstrated a quantum leap forward in analytical potential.

The present work reports an optical near-field biosensor in a planar chip format utilizing Au NP probes for signal generation in a distance-dependent interferometric setup. In contrast to the conventional reflectometry-based surface plasmon resonance (SPR), we describe a biosensor format based on resonance-enhanced absorption (REA) that represents a unique improvement in applicability to biological analysis compared to other direct optical sensors for the following two reasons: first, the use of colloidal gold as a signal transducer within the optical near-field, which allows for detecting signals with the naked eye, and second, the interferometric setup. Besides simple protein binding or DNA hybridization information, the REA optical biochips are also capable of yielding steric information generated via the bioassay.

Subwavelength-sized particles of noble metals and semiconductors exhibit optical resonances (surface plasmons) associated with collective electron oscillations that can be used to monitor changes in the surrounding medium in thin film and size-dependent colloidal metal cluster applications.² Optically active metal NPs have shown excellent applicability to biosensing with respect to protein–protein and protein–ligand interactions. Several techniques have previously been reported that use Au NPs in particular for labeling of DNA^{3–6} and proteins,^{7–11} since the particles do not affect the activity or unique functionality of these

* To whom correspondence should be addressed. Phone: +43 1 4277-52808. Fax: + 43 1 4277-9528. E-mail: irene.maier@univie.ac.at.

[†] University of Vienna.

[‡] Parts of the work were carried out in the course of a temporary stay at the University of Leeds, UK.

[§] University of Leeds.

^{||} University of Vienna.

(1) Kingsmore, S. F. *Nat. Rev. Drug Discovery* 2006, 5, 310–320.

(2) Eustis, S.; el-Sayed, M. A. *Chem. Soc. Rev.* 2006, 35, 209–217.

(3) Elghanian, R.; Storhoff, J. J.; Mucic, R. C.; Letsinger, R. L.; Mirkin, C. A. *Science* 1997, 277, 1078–1081.

(4) Mirkin, C. A.; Letsinger, R. L.; Mucic, R. C.; Storhoff, J. J. *Nature* 1996, 382, 607–609.

(5) Han, M. S.; Lytton-Jean, A. K.; Mirkin, C. A. *J. Am. Chem. Soc.* 2006, 128, 4954–4955.

(6) Han, M. S.; Lytton-Jean, A. K.; Oh, B. K.; Heo, J.; Mirkin, C. A. *Angew. Chem., Int. Ed.* 2006, 45, 1807–1810.

(7) Liang, R. Q.; Tan, C. Y.; Ruan, K. C. *J. Immunol. Methods* 2004, 285, 157–163.

(8) Thanh, N. T.; Rees, J. H.; Rosenzweig, Z. *Anal. Bioanal. Chem.* 2002, 374, 1174–1178.

(9) Thanh, N. T.; Rosenzweig, Z. *Anal. Chem.* 2002, 74, 1624–1628.

biomolecules (which can be problematic for the analysis of the latter). Excitation of localized surface plasmons results in the occurrence of pronounced extinction bands and in local field enhancement effects.¹² The search for configurations ensuring reliable realization of strongly enhanced local fields has often been conducted with the help of linear extinction spectroscopy in two complementary modes, where minimums in the transmitted light intensity were associated with the generated plasmon bands.¹² In the first mode, extinction-based¹³ techniques work on the direct visualization by long-range coupling of surface plasmons in colloidal suspension. Changes in the proximity of the colloids induced by aggregation of the particles can be detected sensitively as changes of the absorbance spectrum.^{5,6,9} A colorimetric detection method for nucleic acids based on the interparticle distance-dependent optical properties of DNA-modified Au NPs was first reported by Elghanian et al.³ In the second mode, the optical signal arises from the dependence of the peak intensity and position of the surface plasmon absorbance of Au NPs upon the local refractive index of the surrounding medium, which is altered due to binding at the colloid–solution interface. First used for DNA monitoring, the strategy of using Au NP bioconjugates was also adopted for proteins. Seelenbinder and colleagues¹⁴ described surface-enhanced infrared absorption spectroscopy of antibodies and antigen/antibody complexes conjugated with colloidal Au particles on porous polyethylene membranes. For the determination of biomolecular binding on a planar surface, Nath et al.¹⁵ described an extinction-based label-free sensor in the second mode format analogous to the conventional SPR technique in total attenuated geometry. Exploiting the ability of colloidal Au to self-assemble on solid substrates, a monolayer of SPR-active Au NPs was immobilized on functionalized glass slides. Again working on a solid support, Li et al.¹⁰ and Su et al.¹¹ reported extinction-based immunoassays using Au NPs for signal amplification in a capture assay. This characterization technique is considered reliable, but lacking in spatial resolution, since the extinction spectra are generally influenced by a whole illuminated area containing many nanoparticles.¹² To overcome these limitations, detection of scattered light as an alternative method increased sensitivity of the colorimetric detection of unamplified genomic DNA sequences with NP probes by over 4 orders of magnitude.¹⁶ However, the arraying of scattered light needs significant instrumentation and, therefore, will not meet the demands of rapid methodology. As a step forward in this course, we sought to develop a one-step homogeneous detection system by directly visualizing (plasmon) resonance-enhanced absorption above a reflecting mirror.

The “golden standard” for monitoring biomolecular affinity binding interactions is immunoassay. For *in vitro* testing, various

protein-detecting array substrates have been described, including nylon membranes, plastic microwells, planar glass slides, gel-based arrays, and beads in suspension arrays.^{17–26} A wide range of formats, using either a single or two antigen-specific antibodies, a labeled detector antibody, or a labeled antigen, have been developed; each format showing both advantages and shortcomings with respect to sensitivity, specificity, and applicability. The herewith reported REA-based immunosensor biochip was applied to the determination of the two allergenic egg white proteins, ovalbumin (OVA) and ovomucoid (OVO),²⁷ in direct and two-site sandwich-type immunoassay format, respectively. Additionally, we demonstrated the successful applicability of the described detection system to the analysis of the target proteins in complex food matrixes that are considered most challenging tasks in bioanalysis.

EXPERIMENTAL SECTION

Materials. OVA (purity $\geq 98\%$) and OVO (trypsin inhibitor, free of ovoidinhibitor) were purchased from Sigma-Aldrich Chemical Co. (Poole, UK), as well as hydrogen tetrachloroauric acid ($\text{HAuCl}_4 \cdot 3\text{H}_2\text{O}$), gelatine from cold water fish skin (45% aqueous solution, containing 0.15% propyl, 0.2% methyl *p*-hydroxybenzoate), poly(vinylpyrrolidone) (PVP), and additional proteins for the cross-reactivity studies (β -lactoglobulin, β -LG; bovine serum albumin, BSA; human serum albumin, HSA; lysozyme, LYZ; α -lactalbumin, LA). Purified IgG-based rabbit antisera against egg white allergens ovalbumin and ovomucoid (anti-OVA PAS-7062 and anti-OVO PAS-8144) and another hen's egg protein, α -livetins, that has been isolated from native and pasteurized egg yolk, were obtained from the Procter Department of Food Science, University of Leeds (UK); Triton X-100 was purchased from Fluka (Buchs, Switzerland). Samples including baby food pasta–cheese and tomato (Cow&Gate, Wiltshire, UK), garlic and herb tagliatelle, and Gooney Toffee Sundae dessert (both Wm Morrison Supermarkets PLC) were commercial products purchased at local stores. All products were labeled as containing egg. Additionally, a whole egg and hydrolyzed egg powder preparation (both pasteurized) by Nestlé (Lausanne, Switzerland) were included. All chemicals used for the preparation of buffers, sample workup, and subsequent immunosensing analysis were purchased from Sigma-Aldrich Chemical Co. (Poole, UK) or Fluka (Buchs, Switzerland) in a purity of analytical grade unless stated otherwise. Target proteins

- (10) Li, H.; Wang, C.; Ma, Z.; Su, Z. *Anal. Bioanal. Chem.* **2006**, *384*, 1518–1524.
- (11) Su, Y.-I. *Appl. Surf. Sci.* **2006**, *253*, 1101–1106.
- (12) Hohenau, A.; Krenn, J. R.; Beermann, J.; Bozhevolnyi, S. I.; Rodrigo, S. G.; Martin-Moreno, L.; Garcia-Vidal, F. *Phys. Rev. B* **2006**, *73*, 155404.
- (13) Niemeyer, C. M.; Mirkin, C. A., Eds. *Nanobiotechnology: concepts, applications, and perspectives*; Wiley-VCH Verlag GmbH: Weinheim, 2004.
- (14) Seelenbinder, J. A.; Brown, C. W.; Pivarnik, P.; Rand, A. G. *Anal. Chem.* **1999**, *71*, 1963–1966.
- (15) Nath, N.; Chilkoti, A. *Anal. Chem.* **2002**, *74*, 504–509.
- (16) Storhoff, J. J.; Lucas, A. D.; Garimella, V.; Bao, Y. P.; Muller, U. R. *Nat. Biotechnol.* **2004**, *22*, 883–887.

- (17) Angenendt, P.; Glöckler, J.; Konthur, Z.; Lehrach, H.; Cahill, D. J. *Anal. Chem.* **2003**, *75*, 4368–4372.
- (18) Huang, R. P. J. *Immunol. Methods* **2001**, *255*, 1–13.
- (19) Schweitzer, B.; Roberts, S.; Grimwade, B.; Shao, W.; Wang, M.; Fu, Q.; Shu, Q.; Laroche, I.; Zhou, Z.; Tchernev, V. T.; Christiansen, J.; Velleca, M.; Kingsmore, S. F. *Nat. Biotechnol.* **2002**, *20*, 359–365.
- (20) de Jager, W.; te Velthuis, H.; Prakken, B. J.; Kuis, W.; Rijkers, G. T. *Clin. Diagn. Lab. Immunol.* **2003**, *10*, 133–139.
- (21) Moreno-Bondi, M. C.; Alarie, J. P.; Vo-Dinh, T. *Anal. Bioanal. Chem.* **2003**, *375*, 120–124.
- (22) Ruiz-Taylor, L. A.; Martin, T. L.; Zaugg, F. G.; Witte, K.; Indermuhle, P.; Nock, S.; Wagner, P. *Proc. Natl. Acad. Sci. U.S.A.* **2001**, *98*, 852–857.
- (23) Pawlak, M.; Schick, E.; Bopp, M. A.; Schneider, M. J.; Oroszlan, P.; Ehrat, M. *Proteomics* **2002**, *2*, 383–393.
- (24) Nallur, G.; et al. *J. Biomed. Microdevices* **2003**, *5*, 117–125.
- (25) Angenendt, P.; Glöckler, J.; Sobek, J.; Lehrach, H.; Cahill, D. J. *J. Chromatogr., A* **2003**, *1009*, 97–104.
- (26) Rubina, A. Y.; Dementieva, E. I.; Stomakhin, A. A.; Darii, E. L.; Pan'kov, S. V.; Barsky, V. E.; Ivanov, S. M.; Kononova, E. V.; Mirzabekov, A. D. *Biotechniques* **2003**, *34*, 1008–1014, 1016–1020, 1022.
- (27) Leduc, V.; Demeulemester, C.; Polack, B.; Guizard, C.; Le Guern, L.; Peltre, G. *Allergy* **1999**, *54*, 464–472.

were used without further purification. Millipore water (18 M Ω cm⁻¹) was used for all reported investigations.

Sample preparation was performed by liquid/solid extraction with phosphate-buffered saline (PBS extraction buffer: 1.5 mM potassium dihydrogen phosphate, 8 mM disodium hydrogen phosphate, 0.14 M sodium chloride). To 30 g of sample, 100 mL of cold PBS extraction buffer was added. The mixture was homogenized for 30 s at low speed with a Waring commercial blender. The samples were then centrifuged at 19000g for 15 min (Beckman high-speed centrifuge, model J2-HS). The supernatant was collected, and aliquots were frozen immediately and kept at -20 °C until required for analysis.

Preparation of Biochips. Polished, hard aluminum foil disks (thickness 0.5 mm, diameter 13 mm, Amag Ranshofen, Austria) served both as mechanical support carriers and as a highly reflective metal mirror layer. The disks were washed with 2-propanol to remove any fatty or organic residues before 100 mL of 38 mg/mL poly(styrene-methyl methacrylate) (PS-PMMA), 70:30, random copolymer, Polysciences, Eppenheim, Germany) in organic thinner (AZ 1500, Hoechst, Frankfurt, Germany) was spin-coated onto the dried surfaces of the disks at 4000 rpm for 12 s using a spin-coater model P 6700 (Speciality Coating Systems, Inc., Indianapolis, IN). Spinning started at 100 rpm for 3 s and was then accelerated to 4000 rpm within 1 s. To monitor the thickness of the distance layer, a 3–5-nm layer of metal clusters was applied on reference chips by sputtering Au with a sputter coater model 108, series 258 (Agar Scientific, Stansted, UK). The outer ring section (Figure 3A) was marked off with an immune-edge pen (Vector Laboratories, Burlingame, CA).

For optical monitoring of results, we used a Polaroid i1032 digital camera (Waltham, MA).

UV-visible spectra of the colloidal Au solutions and Au NP-conjugated readout (detector) solutions were recorded using a U-2000 spectrophotometer (Hitachi, Tokyo, Japan). To estimate and calibrate the visible color development on the chip surfaces after running the immunoassays, a self-focusing reflective grating array spectrometer (VIS LIGA microspectrometer operated with SPEC view3.3 software by STEAG microParts, Dortmund, Germany) was applied to spectrally analyze the absorbance and reflection, respectively.

Preparation of the Au NP-Antibody Conjugate (Au Cluster Detector Solution). Monodisperse, spherical Au NPs with an average size of 16 nm²⁸ were synthesized chemically by the reduction of tetrachloroauric(III) acid with citrate according to the protocol by Frens.²⁹ To 100 mL of boiling 0.01% (w/v) HAuCl₄, 4 mL of an aqueous solution of sterile filtered 1% (w/v) trisodium citrate was added under vigorous stirring. Nanosized citrate-reduced aggregates of Au atoms are formed, referred to subsequently as Au NPs in colloidal suspension, with a negatively charged surface formed by citrate ligands. For REA application, modified Au NPs are renamed Au “clusters” on the basis of forming a thin layer of isolated NPs on a solid support at high density, although they are not accumulated in sol.

For preparing the final readout (detector) solutions, 10-mL aliquots of the colloidal Au NP solution (pH 9) were incubated with appropriate microliter amounts of purified rabbit antisera for

20 min under constant stirring at room temperature (RT). The titer was assessed to be 30 μ L for purified anti-OVA and 70 μ L for anti-OVO antiserum (prediluted 1:10 with water). Finally, Triton X-100 was added to a final concentration of 0.5% (v/v) and the detector solution of Au NP-antibody conjugate then stirred for 30 min. The solutions were centrifuged in a benchtop centrifuge (Eppendorf centrifuge 5415C) at 13 000 rpm (equals 13793g) for 10 min. The clear and almost particle-free aqueous supernatant was taken off, leaving a 50- μ L volume in the tubes to gently resolve the Au cluster pellet. Thus, 10 mL of the conjugated Au NP solution was reduced to a volume of 500 μ L of final Au cluster detector solution.

Confocal Microscopy. A Leica confocal laser scanning microscope was operated in fluorescence mode to examine the microstructure of the samples relating to protein coating. An Ar/ArKr laser source at 488 nm was utilized. The chip surfaces were fluorescence-dyed with a 0.01% (w/v) solution of fluorescein isothiocyanate (isomer I) to highlight the protein-coated sections. Emitted light in a range from 520 to 640 nm was acquired.

RESULTS AND DISCUSSION

Plasmon resonance properties¹² of biofunctionalized Au NPs allow biodetection based on interactions with electromagnetic waves in an advanced layered optical near-field setup. If metal (Au) NPs are undergoing an antigen-antibody binding process within a defined nanodistance (≤ 400 nm) to a highly reflective mirror and illuminated with white light of the visible and near-infrared spectrum from the particle side, they will generate a strong color effect (REA^{30–32}). This optical phenomenon was used to adjust a conventional enzyme-linked immunosorbent assay (ELISA) to a gold cluster-linked immunosorbent assay on a chip by conjugating a Au NP instead of an enzyme to the detector biomolecule.³³ A multilayered resonant system was created for the REA chips as illustrated in Figure 1A. From the bottom to the top, we employed a highly reflective aluminum disk providing the mechanical substrate and mirror, an optically transparent polymeric distance layer, on which solid-phase one and multistep affinity interaction assays are carried out and, finally, a consequent biorecognitively bound metal nanocluster layer for colorimetric readout. In the direct immunosensing format (Figure 1B-1), the surface of the polymeric distance layer was coated with the capture molecule (antigen, in our case: ovalbumin and ovomucoid). Molecular recognition was performed with a single affinity binding step using Au NP-conjugated immunoglobulins (IgG) in a colloidal suspension. If the conjugated antibodies are bound to the immobilized antigen, they will be located within the essential resonance distance, and thus, a blue resonance color will become visible in the shape of a blue dot on the chip, exactly where the allergenic target protein was dotted for coating. In the same way, a two-site or sandwich-type immunoassay was constructed by first precoating the chips with antibodies (Figure 1B-2).

REA biochips exhibited strong reflection minimums as a result of interference of light waves between the mirror layer and the

(28) Li, X.; Yuan, R.; Chai, Y.; Zhang, L.; Zhuo, Y.; Zhang, Y. *J. Biotechnol.* **2006**, *123*, 356–366.

(29) Frens, G. *Nat. Phys. Sci.* **1973**, *241*, 20–22.

(30) Mayer, C.; Stich, N.; Palkovits, R.; Bauer, G.; Pittner, F.; Schalkhammer, T. *J. Pharm. Biomed. Anal.* **2001**, *24*, 773–783.

(31) Bauer, G.; Hassmann, J.; Walter, H.; Haglmueller, J.; Mayer, C.; Schalkhammer, T. *Nanotechnology* **2003**, *14*, 1289–1311.

(32) Haglmueller, J.; Rauter, H.; Bauer, G.; Pittner, F.; Schalkhammer, T. *IEE Proc. Nanobiotechnol.* **2005**, *152*, 53–63.

(33) Hohensinner, V.; Maier, I.; Pittner, F. *J. Biotechnol.* **2007**, *130*, 385–388.

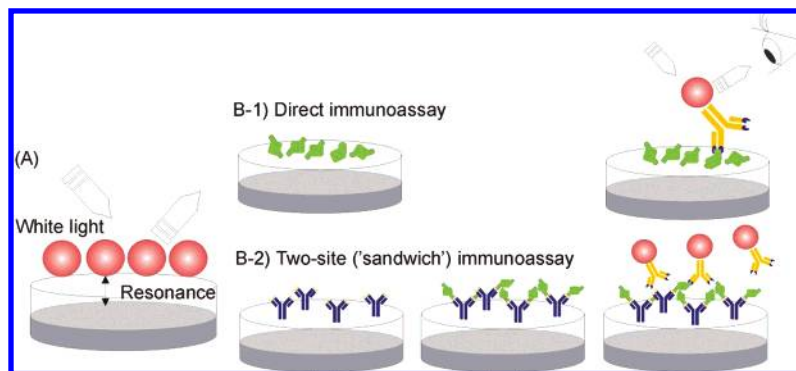


Figure 1. (A) Schematic illustration of the REA setup. The nanoclusters are deposited above a highly reflecting mirror surface. Interlayer distance-dependent light that is reflected by the mirror is in phase with the incident field. Thus, the REA setup acts as a nanointerference filter. (B) Schematic representation of the two immunoassay formats. (B-1) Direct immunoassay. Antigen is immobilized onto the surface of the optically transparent distance layer of the immunochips and screened by Au NP-labeled antibodies. (B-2) Two-site (sandwich) assay. The chips are pre-coated with the first antibody. The antigen is then captured by the antibody and detected with a second Au NP-labeled readout antibody.

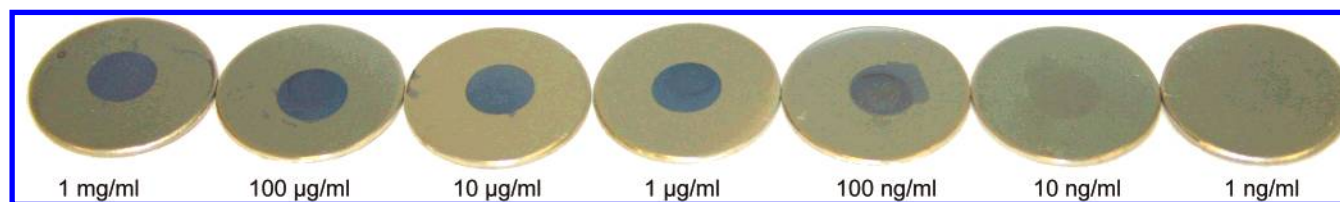


Figure 2. Dynamic range in the direct antigen capture assay. Antigen is determined in a series of 10-fold diluted standard protein solutions ranging from 1 mg/mL to 1 ng/mL concentrations.

biorecognitively captured Au NPs, induced by the resonant absorptive behavior of the latter. Resonance absorption of the mirror-reflected light is phase modulated and therefore inherently determined by the distance between the mirror and the excited nanoclusters of isolated metal NPs on a solid phase. This nanointerference system acts in a similar way to a reflection filter and is angle-dependent due to the incident waves. Its feedback mechanism strongly enhances the absorption coefficient of the metal clusters,³³ which results in a theoretical increase in sensitivity as compared to absorbance-based^{3,10} or recently refined scatter-based methods.¹⁶ For protein detection, the above-mentioned sensitivity increase allows analysis at the low micromolar to nanomolar range. The spectral position of the resonance peak that correlates with the reflection minimum and the developed color on the chip surface relies on the distance between the cluster layer and the mirror surface and can so be utilized to determine changes in thickness of a few nanometers. Whereas the spectral position of the surface plasmon resonance of noble metal NPs depends on many parameters as structural geometry and the polarization state of the excitation light, the size and shape of the particles, and their distance, the type of the presently described REA biochips is characterized solely by the interlayer distance. A multipole resonance effect of the visible spectrum leads to a colorimetric response visually detectable by the naked eye. With increasing thickness of the polymer and the biomolecular interlayer, the spectral position of the REA resonance peak shifts to the red, far away from the plasmon peak of the cluster layer—which for spherical Au NPs in colloidal suspension is at ~520 nm—and additional resonance modes appear in the spectrum (thickness of ≥ 150 nm). Coloring of a chip will occur if Au NP-conjugated biomolecules are bound to the polymer surface of the chip within the optical near-field. Thereby, a special focus was

placed on the fact that the color development on chip (brilliant blue, Figure 3A) was adjusted to be different from the color of the colloidal Au sol (red, Figure 4B). This is the most advantageous setup and the main characteristic property that allowed the REA setup to contribute to an increase in selectivity among Au NP-working biochips. The signal generation is tuned by the optical interference of reflected light in contrast to the use of Au NP probes in colloidal suspension and spot tests,^{3,5,6} or the label-free surface plasmon geometry. Bound and unbound metal cluster labels can be distinguished without any separately performed washing step or further enzymatic reactions for colorimetric readout, thus allowing application of this advanced optical detection system to improve selectivity and simplicity of conventional binding assays. Independent of the spectral position of the resonance absorption, the intensity of the color correlates directly with the number of clusters deposited on the chip surface and, therefore, can be calibrated according to the amount of affinity-captured Au NPs by antigen. For semiquantitative measurements, the chips can be read photometrically.

Biochip Sensor in a Direct Immunoassay Format for the Detection of Ovalbumin and Ovomucoid. As briefly outlined in the Experimental Section, the chip-based mirror was built up from highly polished aluminum disks, which were homogeneously spin-coated with a PS-PMMA copolymer, forming the optical distance layer and solid phase for immobilizing antigens and antibodies, respectively. The viscosity of the polymer solution was associated with the acceleration for spinning and together adjusted to give a violet-blue or brilliant blue resonance color with an absorption maximum at 574 nm measured for the Au sputter-coated positive control reference chip (Figure 3B-2).

We used polyclonal rabbit antisera against OVA and OVO in direct and indirect two-site solid-phase immunoassays on the chips

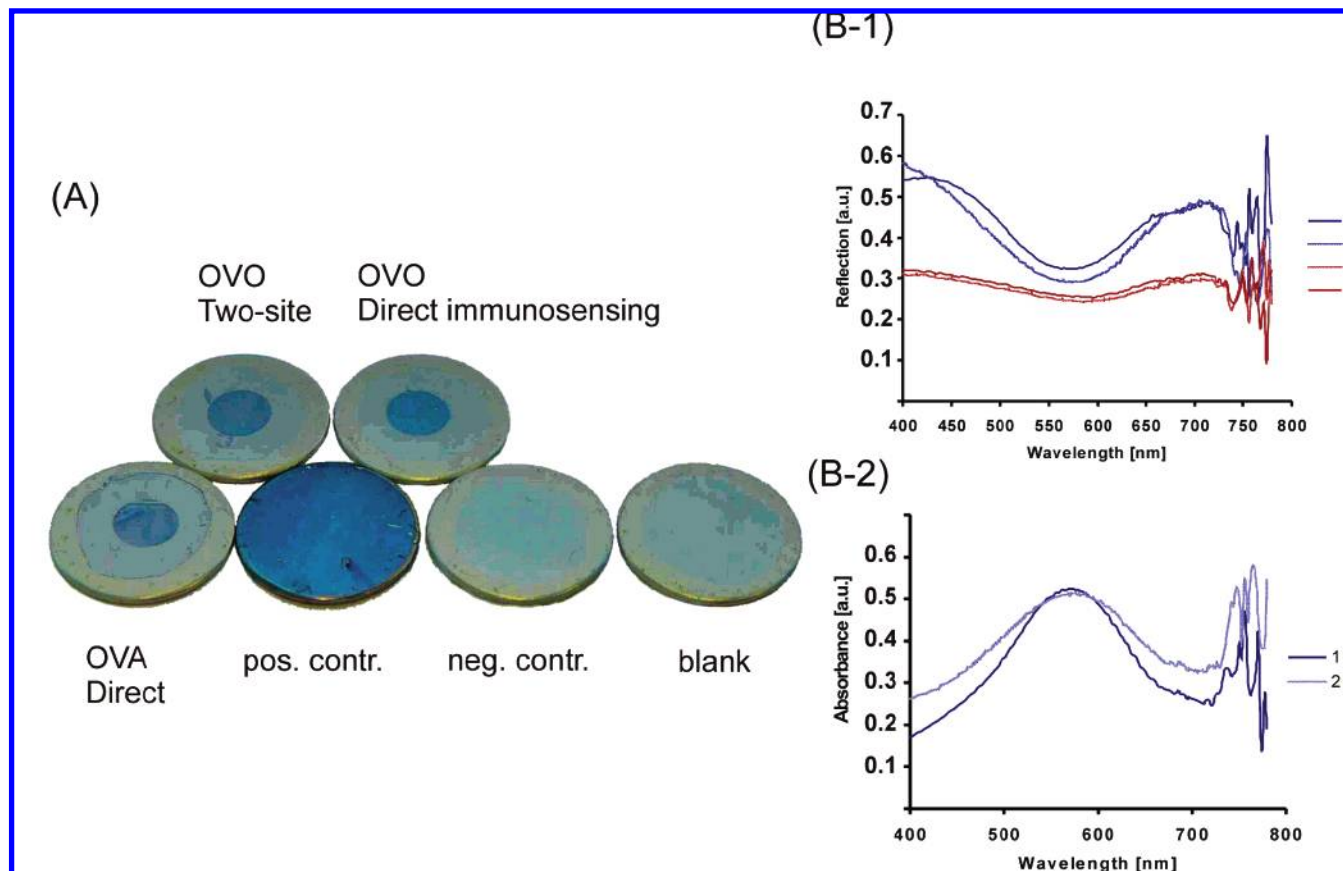


Figure 3. (A) Visually detectable colorimetric signals on chip. The upper line shows two immunochips both detecting 10 $\mu\text{g/mL}$ OVO in two-site (sandwich) and direct immunoassay format. After washing and blocking, the chips were incubated with the Au NP-bioconjugate in colloidal suspension stabilized with Triton X-100. In the two-site sandwich assay, the chip was coated with diluted purified rabbit antiserum (20 μL) before incubation with antigen and final detection with Triton X-100 stabilized and Au NP-conjugated second antibody. In the directly detecting assay, the same procedure was applied as for the OVA chips. The bottom line (from the left to the right) shows an immunochip coated with 10 $\mu\text{g/mL}$ OVA, a Au sputter-coated reference chip as positive control, the negative control incubated with nonfunctionalized colloidal Au cluster solution, and a PBS blank. (B-1) Photometric readout of immunochips detecting OVA in direct assay format. (1)–(3) 10 $\mu\text{g/mL}$ OVA were immobilized on the chip substrates. (1) The chip was incubated with Triton X-100-stabilized detector solution with an antibody titer as given in the Experimental Section (3 μL in 10 mL). (2) The antibody titer for preparing the functionalized detection solution was increased to 5 μL in 10 mL of colloidal Au cluster solution. (3) The chip was incubated with a cluster solution without antibody. (4) PBS blank. PBS buffer pH 7.4 instead of antigen was dotted on the chip surface and incubated with Au NP–anti-OVA IgG-conjugate. (B-2) Resonance-enhanced absorbance spectrum of a sputter-coated film of isolated Au cluster particles (1) and an OVA detecting chip in direct assay format (2). The positive control chip shows the same blue resonance color as the assay performing chips due to the same distance layer applied by polymer spin-coating.

as outlined in Figure 1B. In the direct assay, the capture antigen was immobilized onto the polymer surface of the distance layer by dotting 20 μL of the protein dissolved in 0.01 M PBS, pH 7.4, in the middle of the hydrophobic, ready-to-use PS–PMMA spin-coated aluminum chips. An incubation time with antigen for coating of only 5 min at RT was sufficient to observe a strong and stable signal (after finishing all assay steps as in the following) that was graduated with the antigen concentrations in a dynamic range from 1 ng/mL to 1 mg/mL, with the theoretical limits for the technique being much lower (Figure 2).

Washing/blocking of the chips was performed with 0.1 M PBS (20 mM potassium dihydrogen phosphate, 80 mM disodium hydrogen phosphate, 100 mM sodium chloride) containing 0.1% (w/v) Tween-20 and 0.05% (w/v) fish gelatine under agitation for 10 min at RT in one combined step. The washing was repeated twice in PBS-T without further additions. Subsequently, the detector Au NP conjugate was applied in excess (40 μL /dot, covering the whole chip surface) and incubated overnight (12 h) at 4 $^{\circ}\text{C}$. Au NP–antibody conjugate was stabilized by the use of

the nonionic surfactant Triton X-100 (see below). Finally, the chip substrates were dipped once in PBS-T and water and kept for drying at RT to see the results. The obtained signals were stable for prolonged time periods, and the chips could easily be archived if desired. Applying the procedure as described above, both the PBS blank assayed with IgG-functionalized detector solution and the negative control carried out with an unmodified Au cluster solution applied to the analysis of immobilized analyte protein resulted in chips that were absolutely blank (reference chips in Figure 3A). Compared to the recently published protocol for detecting β -lactoglobulin,³³ unspecific binding of Au clusters to the analyte could be reduced to an absolute minimum.

Concerning the time required for the direct assay performance (total time of analysis), the incubation time with Au NP detector solution can be reduced to 2 h at RT, but should not be performed at 37 $^{\circ}\text{C}$ as this increased the tendency of proteins to interact with the Au NP labels electrostatically and therefore unspecifically. Shorter times at RT will even reduce unspecific binding, but in the same course might also reduce reproducibility and sensitivity

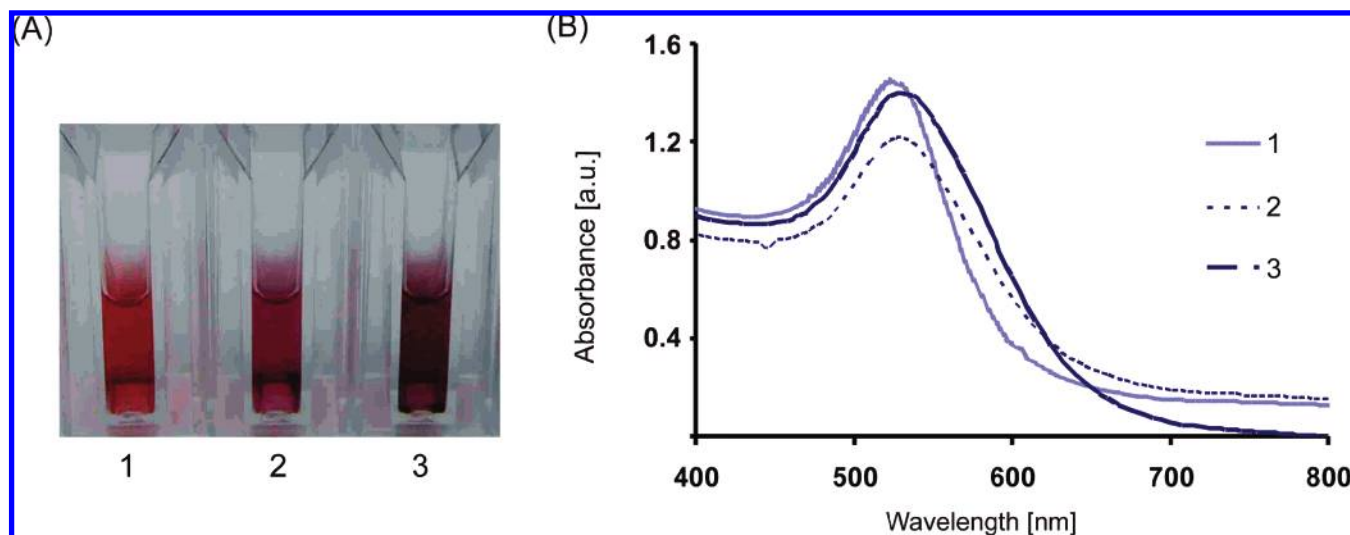


Figure 4. (A) Colloidal Au cluster solutions. (1) Monodisperse Au cluster solution containing 0.5% (v/v) Triton X-100; (2) Anti-OVO antiserum (7 μ L in 10 mL) functionalized Au cluster solution containing 0.5% (v/v) Triton X-100; (3) Anti-OVA antiserum (3 μ L in 10 mL) functionalized Au cluster solution containing 0.5% (v/v) Triton X-100; (1)–(3) Suspensions were diluted 1 in 10 with ddH₂O for measurements. (B) “Normalized” plasmon UV–visible absorbance spectra of the Au cluster solutions shown in (A). Peak maximums are at (1) 524, (2) 529, and (3) 530 nm.

of the test. As to the very short coating time with antigen, another positive factor to emphasize was that we succeeded in reducing the immunochemical cascade of incubation steps to only one, namely, the incubation with Au-labeled antibodies after one combined washing and blocking step.

Sandwich-Type Immunoassay for the Detection of Ovomucoid. Analogously to the simplified direct immunosensing format, a two-site or sandwich assay was successfully set up for the detection of OVO. In the first step, the dot surface on the biochip was coated with the capture antibody (purified rabbit anti-ovomucoid, diluted 1:1000 with PBS buffer) overnight at 4 °C. After washing and blocking the chips in the same way as described above for the direct assay, the whole chip was incubated with antigen for 2 h at RT. Subsequently, the detection was performed as before with Au NP-conjugated antisera overnight at 4 °C.

Figure 3A compares the signal intensities of chips detecting OVA and OVO in the direct assay format applying Triton X-100-stabilized detection solutions and OVO in the two-site format depicted next to a negative and Au sputter-coated positive control. Resonance colors from biorecognitively captured plasmon-generating Au NPs appear exactly where the analyte protein or capture antibody has been dotted onto the chip surface. The assay on the solid support can be developed for the direct immunosensing approach as well as a multistep format of several consecutively applied affinity binding interactions and clearly demonstrates that the response of a REA-based biochip sensor complies for the demands on specific immunochemical monitoring of the analyte protein. Graphs showing the reflection minimums of the OVA detecting biochips are shown in Figure 3B-1. It has to be mentioned that the minimal absorbance measured on cluster-free chips at \sim 589 nm results from the refractive index of the PS–PMMA distance layer itself. In full agreement with the REA peak maximum of the Au sputter-coated reference chip at 570 nm, the blue dots showed a reflection minimum at 568 nm. However, when the antibody concentration in the detection solution was further increased, the signal appeared to be more intense, but less bright, because of a multilayer of Au clusters bound that diminished the

resonance effect. At the same time, the spectrum for these chips slightly and very sensitively shifted to the red and showed the reflection minimum at 577 nm.

Au NP–Antibody-Bioconjugate. Typically, the wet chemical preparation of the Au NPs is carried out in the presence of anionic components (in our case citrate ligands), which bind to the atoms exposed at the surface of the NPs forming a negatively charged shield. This capping leads to a stabilization and prevents uncontrolled growth and aggregation of the NPs by repulsive actions.³⁴ The actual spontaneous coupling of Au NPs to biomolecules relies on the combined effects of chemisorption of thiol-containing residues to the gold by ligand-exchange reaction. This highly depends on the pH environment and the size of the particles due to steric hindrance to achieve an effective immunological labeling. The strong affinity of Au particles (using unprotected Au NPs for most sensitive plasmon resonance properties) to proteins poses the problem of unspecific binding to any other components of the bioassay system, e.g., protein targets, in the same way. In complex setups, the electrostatic environment may dominate the required specific biomolecular interaction between antigen and antibody. An inert macromolecule such as BSA is therefore often added to the bioconjugate of Au NP and antibody to block undesired charged Au NPs,¹⁰ usually before addition of the antisera, showing the additional effect of stabilization. In this study, we added only antisera, first. The optimal coupling ratio was determined by means of flocculation assay.³⁵ Second, BSA (0.5%, w/v), fish gelatine (0.1–0.5%, w/v), Tween-20 (0.5%, v/v), and Triton X-100 (0.5%, v/v) were added to the cluster detector solutions and tested for response to the appropriate antigen through dot blot analysis on nitrocellulose membranes and on the biochips. The given methodology for blocking the functionalized cluster solutions predominantly influenced the affinity

(34) Niemeyer, C. M. *Angew. Chem., Int. Ed.* **2001**, *40*, 4128–4158.

(35) Xie, H.; Tkachenko, A. G.; Glomm, W. R.; Ryan, J. A.; Brennaman, M. K.; Papanikolas, J. M.; Franzen, S.; Feldheim, D. L. *Anal. Chem.* **2003**, *75*, 5797–5805.

binding to the antigen and the interaction behavior with the solid support.

In the negative controls, HSA and lysozyme were used. As the isoelectric point of lysozyme is at about pH 11, this protein shows very strong positive charges under working conditions. Thus, it provides an ideal "catcher" antigen for checking the effect of a simple gold stain due to unspecific ionic interaction between insufficiently blocked Au clusters and the immobilized protein. Each blocking reagent used for the detector solutions was also studied for blocking unoccupied binding sites on the membranes and biochips in correlation with itself and all the other reagents listed: 2% (w/v) BSA, 2% (w/v) fish gelatine, 1% (w/v) PVP, 0.5% (v/v) Tween-20, and 0.5% (v/v) Triton X-100. Additionally, 2% (w/v) skimmed milk powder was applied for blocking binding sites on assay substrates. The use of BSA or skimmed milk powder seemed to be obvious as it is the most frequently used blocking agent for all immunochemical methods, but both stuck to the hydrophobic surfaces where the target proteins had already been immobilized before. When the proteins were applied without any surfactant in the blocking buffer, they completely covered the chip surface. Thereby, any further specifically programmed interaction with the biofunctionalized conjugate was inhibited, especially in the simplified direct assay format where only two molecules were involved in the biomolecular interaction in close vicinity to the solid surface.

In terms of the additives' capacity of blocking the Au clusters, proteins and protein-containing formula are generally quite big attributes to the "label" of a 16-nm-sized Au NP, which itself is a huge carrier for antibodies in a binding assay. The size of the Au NPs was optimized to be ~16 nm in order to balance the problems larger particles may cause due to steric hindrance and low diffusion factors and the limitations of generating a strong REA effect if the metal NPs used were too small. Electrical and optical properties of Au NPs are size-dependent relating to the extent of energy being piped into an excited metal particle. Regarding the blocking reagent, no or insufficient signals were obtained for BSA, skimmed milk powder, and fish gelatine by testing for egg allergens, although fish gelatine proved blocking ability when tested with lysozyme and compared with the respective antigen on the biochip surface. Fish gelatine and PVP used as blocking reagents for the nitrocellulose membrane yielded a strong background signal. By contrast, when low concentrations of fish gelatine (0.05% w/v) were added to the PBS-T washing buffer, fish gelatine applied for the biochip assay reduced unspecific binding and showed no interaction with the modified cluster solutions.

Consequently, the blocking reagent was a low molecular weight inorganic molecule such as a nonionic detergent rather than a macromolecule. Triton X-100 and Tween-20 did not really block the cluster solution, but stabilized the colloidal solution and facilitated the concentration step during centrifugation. On the nitrocellulose, membrane-specific signals were obtained for the respective antigen, but also weak signals for the control proteins. Interestingly, the specificity and intensity of signals was determined by the antibody titer for the cluster detection solution (data not shown). The more antibodies added to the cluster solution, the less unspecific cross-reactivity with proteins was observed. Therefore, the blocking of the charged Au NP surface was

restricted to the use of a maximum amount of antibodies up to a limit when precipitation of the Au NPs occurred. Working in a plateau range with IgG-saturated Au clusters should minimize the effects of signal intensity variations due to inhomogeneous antibody distribution. (Exact titers were examined for each antisera used, separately.) Moreover, this effect indicates high labeling efficiency and that the antibodies adsorbed to the Au NPs retained full activity. Dissociated antibodies could not be detected in the supernatant after centrifugation of the modified Au NP conjugate.

In conclusion, with 0.5% (v/v) Triton X-100 as an additive to the IgG-saturated Au cluster solution, a subsequently applied concentration step allowed production of the final detector solution and further did not interfere with the antigen-antibody interaction in an inhibiting way. Its nonpolar properties stabilize the interaction with hydrophobic areas on biomolecules by partially minimizing hydration complexes at the local microenvironment, and thus supported interactions with the immobilized antigen.

Figure 4A shows the colloidal solution of 16-nm mean-sized Au NPs with Triton X-100 compared to the IgG-modified detection solutions for OVA and OVO. High amounts of antisera appeared in a color change from red to purple. Absorbance spectra of these detection solutions are matched and qualitatively compared in Figure 4B. The binding of antibodies to the Au clusters resulted in slightly broadened plasmon peaks and a red shift of the maximum in absorbance, but did not interfere with the stability of the suspension. They remain stable and immunologically active at 4 °C for months.

Protein Adsorption Behavior. Polystyrene materials, including pure polymers, polymer blends, and copolymers, are extensively applied in biomedical and pharmaceutical research as substrates and carrier materials. Polystyrene is usually used for the fabrication of microplates predominantly used for immunoassaying, where immobilization of biomolecules mostly relies on hydrophobic interaction and the amount of binding sites of the antigen. Despite the drawback of being an analyte-dependent immobilization technique performed in a completely uncontrolled way, our findings might refute ideas concerning inefficient degrees of protein adsorption, even for small proteins. The use of chemically modified surfaces, as recently demonstrated,¹⁰ is not proven to increase the binding capability of assay substrates, although may be arguing for being less dependent on the nature of the biomolecule to be immobilized. Surface chemical structures and surface morphology, however, can mediate protein adsorption behavior. Recently, adsorption behavior has been extensively studied by X-ray photoemission electron microscopy³⁶ and sum frequency generation vibrational spectroscopy,³⁷ as well as atomic force microscopy. Copolymers showed more flat surfaces and intermediate homogeneous properties concerning hydrophobicity than the blends by investigating the selective adsorption of fibrinogen on either the copolymer or different blends of PS and PMMA. It cannot be excluded that proteins show time-dependent structural and orientational changes after being absorbed onto the polymer. Johnson et al.³⁷ clearly demonstrated that the use of different polymer compositions can affect proteins differently. For

(36) Morin, C.; Hitchcock, A. P.; Cornelius, R. M.; Brash, J. L.; Urquhart, S. G.; Scholl, A.; Doran, A. J. *Electron Spectrosc. Relat. Phenom.* **2004**, *137*–140, 785–794.

(37) Johnson, W. C.; Wang, J.; Chen, Z. J. *Phys. Chem. B* **2005**, *109*, 6.

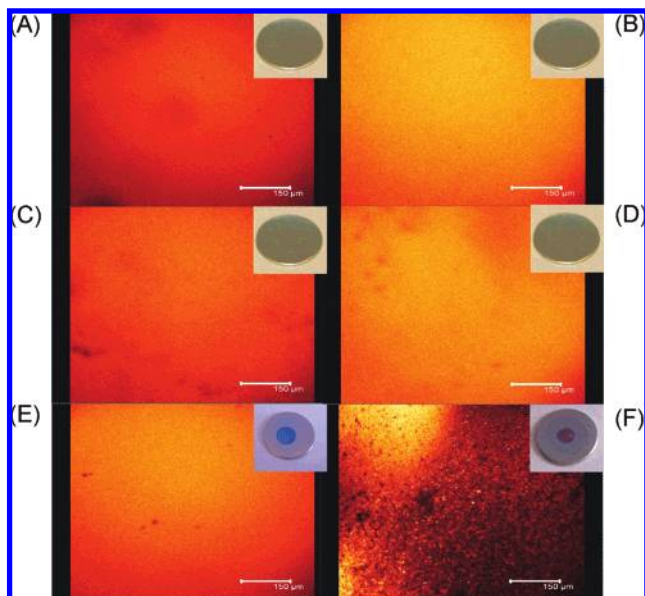


Figure 5. Imaging of fluorescence-dyed antigen-coated chip substrates by confocal microscopy. (A) The chip was coated with 10 $\mu\text{g}/\text{mL}$ OVA in 0.1 M PBS-T buffer, pH 7.4, containing 0.05% (v/v) Tween-20. (B) Coating was performed with OVA (10 $\mu\text{g}/\text{mL}$) in 0.01 M PBS buffer, pH 7.4. (C) The chip was coated with 10 $\mu\text{g}/\text{mL}$ OVA in 0.1 M PBS-T buffer pH 7.4 containing 0.05% (v/v) Tween-20 as in (A), and subsequently washed 3 times for 10 min with washing buffer (PBS-T). (D) Coating was performed as in (B), and 3 washing steps were applied as in (C). (E) Coating was performed as in (B); after washing and blocking, the chip was incubated with Triton X-100-stabilized anti-OVA IgG-conjugate overnight at 4 $^{\circ}\text{C}$. (F) Au cluster precipitation.

our bioassay, however, the effect to diminish the activity and susceptibility of epitopic sites as a consequence of the immobilization step performed prior to the actual detecting recognition of bioconjugated Au NPs can be neglected. We applied only very short time periods and did not observe any problems relating to the binding of either ovalbumin (average size of 42.7 kDa and pI of 4.5), ovomucoid (28 kDa; pI of 4.1),²⁷ or the very small whey protein β -lactoglobulin (18.4 kDa; pI of 5.3), or any other protein applied for the cross-reactivity studies to be immobilized on the PS-PMMA substrates at analyte concentrations of the low millimolar range. To confirm this surprising finding, protein binding was studied by confocal microscopy operated in the fluorescence mode. Ready-to-use PS-PMMA spin-coated chip substrates were incubated for less than 1 min with the antigen OVA (10 $\mu\text{g}/\text{mL}$) dissolved in either PBS-T or PBS. The following aspects were studied for positive and negative effects to estimate the binding capacity of protein to the PS-PMMA surface: the use of different coating and washing buffers with request to their ionic strength and the addition of the detergent Tween-20. It was obvious that almost no protein binding occurred applying the PBS-T buffer, whether the chips were washed 3 times for 10 min with PBS-T after coating or not (Figure 5A+C). The fluorescence-dyed chips appeared very dark. By contrast, homogeneously bright chips representing protein binding were observed when a PBS-buffered antigen solution had been in contact with the hydrophobic polymer for only seconds (Figure 5B+D). The results were unaffected by subsequent washing steps carried out 3 times with PBS-T for 10 min. As expected, the binding of Triton X-100-stabilized Au cluster conjugate did not change the micro-

scopic appearance of a stable REA-active layer of isolated Au clusters because of insufficient optical resolution (Figure 5E). A chip with clotted Au precipitation was added for comparison (Figure 5F).

The requirements for efficient protein binding are manifold and include the contribution to stability of the protein as well as providing an optimum microenvironment by ionic and pH conditions. The sample volume was adjusted to yield a colored dot of a size not too small, so that it could be read out photometrically, and not too large for the economical use of reagents. Sample volume, dot size, incubation time, and sensitivity act in concert, although in parallel every analytical parameter must be optimized for the final assay conditions considered individually and collectively. High reproducibility was a result of excellent binding capacity, protein stability, assay specificity, and a good balance of physical properties of the PS-PMMA support, the immobilized antigen, and the Au NP label with the help of directly applied surfactants.

For the present method, 20- μL aliquots of protein standard solution and food sample extracts were used for immobilization of target proteins onto the polymeric solid support. Given the fact that the signal intensities could be correlated directly with the concentration of analyte protein, and the signal intensities are not dependent on the volume of the sample liquid or size of the dots, we propose that only molecules in proximity to the surface are immobilized. Only a small portion of analyte molecules contributes to the signal. Sensitivity as a result might be limited, but assuming that we measure the actual analyte concentration of only a monolayer of protein immobilized onto the solid-phase support, this, on the other hand, allows for calibrating the detection over a wide dynamic range.

Cross-Reactivity with Different Protein Compounds of Complex Food Matrixes. Regardless of the bioassay construction that provided blank negative controls, low cross-reactivity might remain due to the first antibody specificity. Cross-reactivity experiments were carried out using a range of commercially available egg proteins and several globular proteins similar to the target allergens OVA and OVO. The specificity of the anti-OVO antibodies used for the two-site ELISA was determined by the new developed immuno chip analysis in direct immunoassay format (Figure 6A) and a second immunochemical rapid dipstick assay to allow comparison of the results (data not shown). Egg proteins (ovomucoid, ovalbumin, lysozyme, pasteurized α -livetin, and nonpasteurized native α -livetin) and bovine milk proteins (serum albumin, α -lactalbumin, β -lactoglobulin) and the reference protein human serum albumin were immobilized on chip substrates at a concentration of 1 mg/mL and incubated with the purified anti-OVO polyclonal rabbit antiserum-conjugate overnight at 4 $^{\circ}\text{C}$ following the technical procedure described above. As shown in Figure 6A, the biochip analyses showed high cross-reactivity with ovalbumin and pasteurized α -livetin and low cross-reactivity with lysozyme and also the milk protein β -lactoglobulin. It is interesting to point out that the cross-reactivity with the pasteurized α -livetin was observed for other antibodies, too. It was suggested that the pasteurization process has an effect on the protein components in egg, which may cause the observed cross-reactivity at the molecular level. In addition, to test the feasibility of the immuno chip biosensor construction as well as the assay

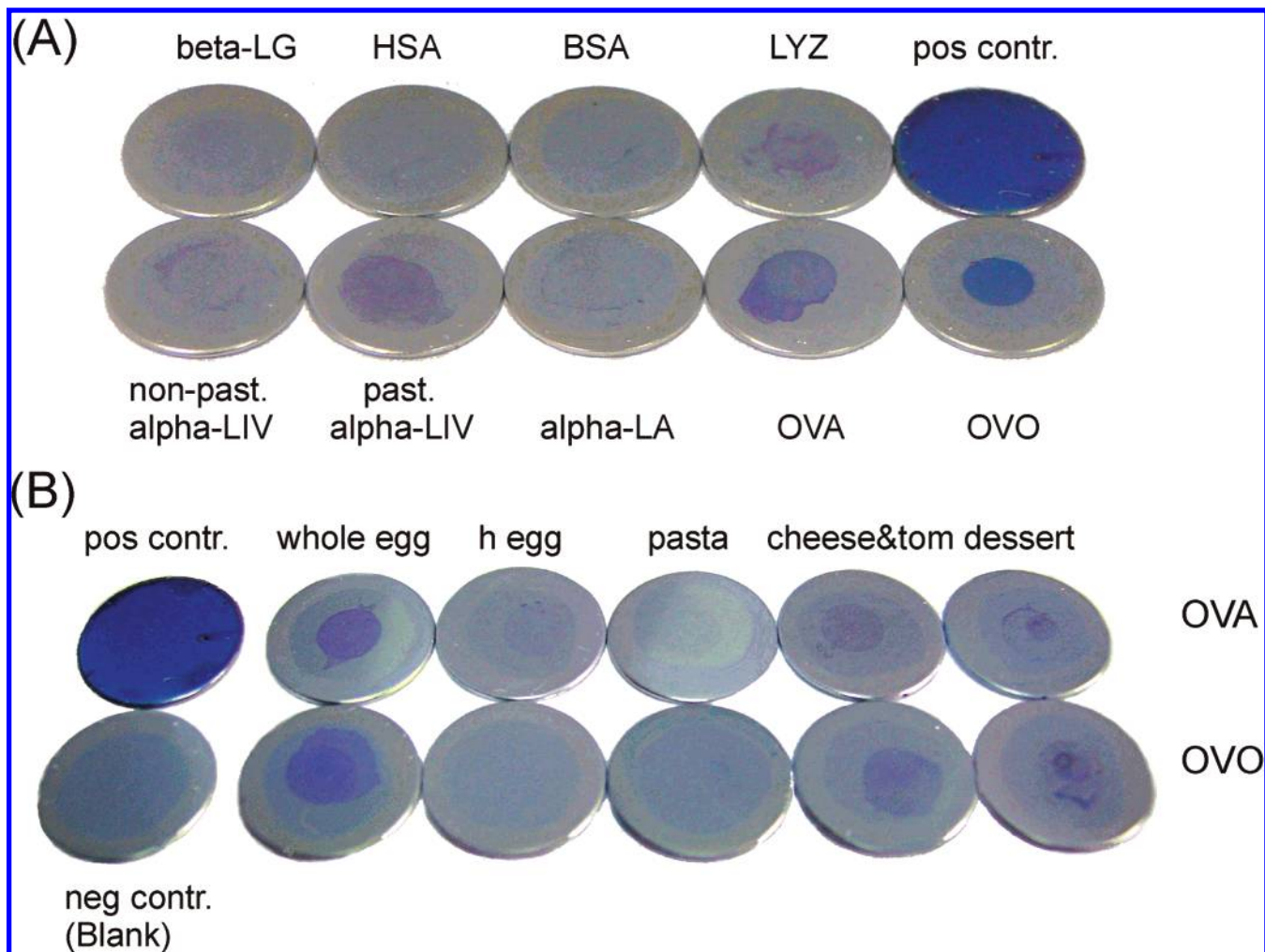


Figure 6. (A) Cross-reactivity studies for anti-OVO antiserum. The chip substrates were coated with reference proteins (β -lactoglobulin, human serum albumin, bovine serum albumin, lysozyme, nonpasteurized α -livetin, pasteurized α -livetin, ovalbumin), and the analyte protein ovomucoid. All protein solutions were applied with a concentration of 1 mg of protein/mL. After washing and blocking, the chips were incubated with Triton X-100-stabilized Au NP-anti-OVO IgG conjugate. (B) Determination of allergenic OVA and OVO in complex food matrixes with the immuno chip sensor. PBS extractions of the samples were diluted 1 in 1000 with 0.1 M PBS buffer, pH 7.4, and immobilized on the chip substrates. After washing and blocking, each sample-coated chip was assayed with Triton X-100-stabilized detection solution for OVA and OVO, respectively. For the blank, PBS buffer instead of protein was dotted onto the chip and the assay also performed with IgG-functionalized Au cluster solution. (A) + (B) As positive control the reference chip was Au sputter-coated.

procedure, several commercial products containing egg (pasta, baby food, and the dessert), a whole egg powder and a hydrolyzed egg preparation (both pasteurized) were investigated. PBS extracts of the samples were diluted 1 in 1000 with 0.1 M PBS buffer, pH 7.4, and assayed with conjugated anti-OVA and anti-OVO antisera, respectively. Semiquantitative results are depicted in Figure 6B. In the whole egg powder and the baby food pasta cheese and tomato, both OVO and OVA were positively detected; also the signals obtained for the extracts of the "dessert" had recognized traces of both egg white allergens. Interestingly, the tagliatelle (pasta) that were also labeled to contain egg (4%) showed no signal. The production process for pasta is known to lead to considerable difficulties in extracting recognizable proteins, even under harsh conditions. For the hydrolyzed dried egg powder, the chips showed a highly reduced level of immunochemical response in comparison with the whole egg due to the extent of hydrolysis. Methods of analysis for proteins in highly processed matrixes (as exemplified by food) have improved significantly in

recent years. Indeed, progress in analysis of food proteins (predominantly through immunochemical methods) has been a major success for analytical science. However, it has become clear as methods have improved that major effort is required to increase understanding of extraction procedures able to provide high yields of protein in a common state of conformation.

Summing up, both OVA and OVO could be detected specifically in complex food matrixes, but the results should be considered as semiquantitative at present. Although the responses were in good agreement with complementary results obtained by a conventional enzyme-linked immunosorbent assay performed in microtitration plate, calibration will need more investigation of the dynamic range, particularly for the millimolar and micromolar range to distinguish between the intensities of color development. The assessment of reliability and, generally, the feasibility of the sensor to test allergenic content of trace amounts in complex food matrixes, however, can be reported as validated with a highly predictive value of positive results and no false-negative responses

above the limit of detection. It was more problematic to define false-positive results due to unspecific interaction of Au clusters with matrix compounds, thereby using complementary analysis methods and different negative controls for cross-validation.

CONCLUSIONS

We have described a simple, rapid, sensitive, and cost-efficient immunochip biosensor methodology based on resonance-enhanced absorption that can be performed in a screening mode. Combined with visual readout that eliminates complex detection instrumentation, this assay system excellently meets the requirements of a simple method for allergen detection and provides opportunities for the development of a miniaturized multiarray sensor with improved sensitivity under nondenaturing conditions for allergy testing in clinical diagnosis.

In this respect, we focused on the evaluation of a simplified assay format directly detecting the target allergens. Selectivity and sensitivity are competitive with common ELISA techniques and may even detect trace amounts of allergenic contents. The final procedure proved applicability for both tested allergens—OVA and OVO—that are different in structure and properties, with reproducible results. Additionally, an indirect two-site im-

munoassay was constructed toward the development of screening tests with IgE of patient sera, which makes it necessary to set up a multilayer incubation assay. We successfully established an optical immunochip biosensor and applied the developed methodology to the rapid detection of two allergenic marker proteins in complex processed and nonprocessed egg-containing food products.

ACKNOWLEDGMENT

This work was cosponsored by UNESCO and L'Oréal giving an international fellowship to I.M. Part of the work was carried out within the EU funded REDALL project (Project QLK1-CT-2002-02687). Both are gratefully acknowledged for giving the grant. We also thank Hassan Firoozmand for providing the microscopic measurements carried out at the Procter Department of Food Science, University of Leeds, UK.

Received for review October 12, 2007. Accepted January 22, 2008.

AC702107K